EAI Endorsed Transactions
on Mobile Communications and Applications
Research Article ICST.ORG

A Unified NET-MAC-PHY Cross-layer Framework for Performance Evaluation of Multi-hop Ad hoc WLANs*

Rachid El-Azouzi[1], Essaid Sabir[2,*], Mohammed Raiss-El-Fenni[1] and Sujit Kumar Samanta[1]

[1]LIA-CERI, University of Avignon, 339 chemin des Meinajaries, Agroparc BP 1228, Avignon cedex 9, France.
[2]RTSE team., GREENTIC/ENSEM, Hassan II University, Route d'El Jadida BP 8118 Oasis, Casablanca, Morocco.

Abstract

Most of the existing works have been evaluated the performance of 802.11 multihop networks by considering the MAC layer or network layer separately. Knowing the nature of the multi-hop ad hoc networks, many factors in different layers are crucial for study the performance of MANET. In this paper we present a new analytic model for evaluating average end-to-end throughput in IEEE 802.11e multihop wireless networks. In particular, we investigate an intricate interaction among PHY, MAC and Network layers. For instance, we incorporate carrier sense threshold, transmission power, contention window size, retransmissions retry limit, multi rates, routing protocols and network topology together. We build a general cross-layered framework to represent multi-hop ad hoc networks with asymmetric topology and asymmetric traffic. We develop an analytical model to predict throughput of each connection as well as stability of forwarding queues at intermediate nodes in saturated networks. To the best of our knowledge, it seems that our work is the first wherein general topology and asymmetric parameters setup are considered in PHY/MAC/Network layers. Performance of such a system is also evaluated through simulation. We show that performance measures of the MAC layer are affected by the traffic intensity of flows to be forwarded. More precisely, attempt rate and collision probability are dependent on traffic flows, topology and routing.

Received on 29 March 2014; accepted on 14 May 2014; published on 24 September 2014

Keywords: Ad hoc network, Performance Evaluation, Cross-layer architecture, Fixed point, Coupled systems.

doi:10.4108/mca.1.4.e6

1. Introduction

In next-generation wireless networks, it is expected that the IEEE 802.11 wireless LAN (WLAN) will play an important role and affect the style of people's daily life. Further, many factors and applications have made the 802.11 wireless LAN networks an attractive commercial field. The low cost of wireless-network interface was the first encouragement to make the network feasible for civilian applications. The distributed nature of the network and the flexibility that provides were the basis of many interesting applications that do not really need maintenance and reconfiguration.

There are lot of interests in modeling the behavior of the IEEE 802.11 DCF (Distributed Coordination Function) and studying its performances for both architectures: the WLAN networks and multi-hop wireless networks. A medium access control protocol has a large impact on the achievable network throughput and stability for wireless ad hoc networks. So far, the ad hoc mode of the IEEE 802.11 standard has been used as the MAC protocols for MANETs. This protocol is based on the CSMA/CA mechanism in DCF.

Over the last decade, there has been a tremendous wave of interest in the study of cooperation in wireless networks, more precisely in wireless ad hoc networks. For instance, the interest has been growing since the publication of famous article of Bianchi [5]. In ad hoc networking context, each neighbor node could assist in the ongoing transmission by exploiting the broadcast nature of the wireless medium. Unfortunately, almost all these studies have been focused on MAC layer without taking into account routing and cooperation level of nodes in ad-hoc networks, see e.g. [1–4, 10, 14–16]. In multi-hop ad hoc networks, the majority of efforts are concentrated on extending Bianchi's model in saturated networks. Now, problem of hidden terminals and channel asymmetry are still real issues for multi-hop ad-hoc networks. Yang et al. [16] proposed an extension of Bianchi's model [5] and Kumar et al. [8] for multi-hop context under symmetric scenario. They studied the impact of carrier sensing range and the transmission power on the sender throughput. The PHY/MAC impact is clearly presented. Basel et al. [1]

*Corresponding author. e.sabir@ensem.ac.ma

have also interested in tuning the transmission power relatively to the carrier sense threshold. They offered a detailed comparison performance between the two-way handshake and the four-way handshake. A three dimensional Markov chain is proposed in [12] to derive the saturation throughput of the IEEE 802.11 DCF. The collision probability is now a function of the distance between the sender and its receiver. The unsaturated node state and the channel state are introduced in [2]. A performance analysis is performed for a single-hop case and a multi-hop case considering that a node can carry different traffic loads. Medepalli et al. [10] proposed an interesting framework model for analyzing throughput, delay and fairness characteristics of IEEE 802.11 DCF multi-hop networks. The applicability of the model in terms of network design is also presented.

Recently, Zhu et al. [17] proposed two cooperative energy efficient algorithms to control the network topology. The authors addressed the problem of inefficient routes that occurs when maintaining the network connectivity, minimizing the transmission power of each node but ignoring the energy-efficiency of paths in constructed topologies. An ordinal potential game formulation is proposed by Chu et al. [19]. They proposed a cooperative approach to determine the transmission power for each node so that it can periodically adapt to the remaining energy on the nodes within its neighborhood. Existence of Nash equilibrium for the game is shown and an algorithm which achieves such equilibrium is proposed. The authors also shown, by simulation, that their algorithm is able to improve the lifetime of a wireless sensor network by more than 50% compared to the best previously-known algorithm. Li et al. [18] studied the throughput of a type of heterogeneous networks consisting of a primary network of size n and a cognitive radio ad hoc network of size m. The authors shown that the individual throughput of a primary user scales is $\Theta\left(1/\sqrt{n}\right)$ with no performance loss due to scaling law. The same result apply for cognitive/secondary users, i.e., the individual throughput scales is $\Theta\left(1/\sqrt{m}\right)$.

Our major goal in this paper, is to build a complete framework to analyze multi-hop ad hoc networks under general and realistic considerations. We present a probabilistic but rigorous model incorporating jointly Network, MAC and PHY layers in a simple cross-layered architecture in a saturated network. This cross-layered architecture has a potential synergy of information exchange among different layers, instead of the standard OSI non-communicating layers. Without any restriction on the network topology, our model is built and valid for any ad hoc network topology under saturation condition. Note that under asymmetry scenario, nodes do not have the same channel perception. Thus, the attempt rate may not always describe the real channel access activity. Moreover, our model is extended to the IEEE 802.11e[1] which provides differentiated channel access (differentiated priority/QoS) to packets by allowing different rates and different back-off parameters. In order to handle QoS, several traffic classes are also supported. We also allow that each traffic/stream may have different retry limits after which the packet is dropped. By analyzing the model, we find that the performance measures of MAC layer may be drastically affected by the routing policy and the traffic intensity of crossing flows. Henceforth, the attempt rate and collision probability are dependent on the traffic flows, topology and routing. From analytical result and as confirmed by simulation, the end-to-end throughput is independent of cooperation level when all forwarding queues are stabled. Hence there is no throughput-delay tradeoff that can be obtained by changing the forwarding probabilities. A real tradeoff is caused by the maximum number of attempts or power control. Indeed, the throughput is ameliorated when reattempting many times on a path, while the service rate on a forwarding queue is slowed down causing low stability region and delay will be increased. A direct application of our work is to find new distributed schemes for channel access and routing that work near optimal stability region of the network.
The structure of the paper is as follows : We formulate the problem in Section 2. Then we derive the expression of end-to-end throughput and stability that determines traffic intensities in the whole network in Section 3. We illustrate our results by some numerical examples in Section 4 and conclude the paper in Section 5.

2. Problem formulation

2.1. Overview on IEEE 802.11 DCF/EDCF

The distributed coordination function (DCF) of the IEEE 802.11 is based on the CSMA/CA protocol in which a node starts by sensing the channel before attempting any packet. Then, if the channel is idle it waits for an interval of time, called the Distributed Inter-Frame Space (DIFS), before transmission. But, if the channel is sensed busy the node defers its transmission and waits for an idle channel. In addition, to reduce collisions of simultaneous transmissions, the IEEE 802.11 employs a slotted binary exponential back-off where each packet in a given node has to wait for a random number of time slots, called the back-off time,

[1] We believe that our model could apply for the recent IEEE 802.11n and the future standard IEEE 802.11ac by integrating the adaptive coding and modulation scheme and the Multiple Input Multiple Output technique as well.

before attempting the channel. The back-off time is uniformly chosen from the interval $[0, W-1]$, where W is the contention window that mainly depends on the number of experienced collisions. The contention window W is dynamic and given by $W_i = 2^i W_0$, where i represents the stage number (usually, it is considered as the current retransmission attempt number) of the packet, and W_0 is the initial contention window. The back-off time is decremented by one slot each time when the channel is sensed idle, whereas freezes if it is sensed busy. Finally, when the data is transmitted, the sender has to wait for an acknowledgement (ACK) that would arrive after an interval of time, called the Short Inter-Frame Space (SIFS). If an ACK is not received, the packet is considered lost and a retransmission has to be scheduled. When the number of retransmissions expires, the packet is definitively dropped. To consider multimedia applications, the IEEE 802.11e uses an enhanced mode of the DCF called the Enhanced DCF (EDCF) which provides differentiated channel access for different flow priorities. The main idea of EDCF is based on differentiating the back-off parameters of different flows. Thus, priorities can be distinguished different initial contention window, different back-off multiplier or different inter-frame space. An Arbitration IFS (AIFS) is used instead of DIFS. The AIFS can take at least a value of DIFS, and, a high priority flow needs to wait only for DIFS before transmission to the channel. Whereas a low priority flow waits for an AIFS greater than DIFS. In the next paragraph, we used a generalized model of the back-off mechanism.

2.2. Problem modeling and cross-layer architecture

The network layer of each node i handles two queues, see Fig. 1. The forwarding queue F_i carries packets originated from some source nodes and destined to some given destinations. The second one is Q_i which carries own packets of node i itself. We assume that the two queues have an infinite storage capacity. Packets are served with a first in first served fashion. When F_i is not empty, the node chooses to send a packet from F_i with a probability f_i, and it chooses to send from Q_i with probability $1 - f_i$. When node i decides to transmit from the queue Q_i, it sends a packet destined to node d, $d \neq i$, with probability $p_{i,d}$. This parameter characterizes somehow the QoS (Quality of Service) required by initiated service from upper layers. We consider that each node has always packets to be sent from queue Q_i, whereas F_i maybe empty. When F_i is empty, the node i chooses to send a packet from the non empty queue Q_i with probability 1. Consequently, the network is considered saturated and mainly depends on the channel access mechanism. In ad hoc networks, each node behaves as a router. At each time, it has a packet to be sent to a given destination and starts by finding the next hop neighbor where to transmit the packet. Clearly, each node must carry routing information before sending the packet. Proactive routing protocols such as the Optimized Link State Routing construct and maintain a routing table that carries routes to all nodes of the network. To do so, it has to send periodically some control packets. These type of protocols correspond well with our model, especially since Q_i is non-empty. Here, nodes form a static network where routes between any source s and destination d are invariant. To consider routing in our model, we denote the set of nodes between a source s and destination d (s and d not included) by $R_{s,d}$. Each node in our model can handle many connections on different paths. The traffic flow leaving a node i is determined by the channel allocation using IEEE 802.11 EDCF. However, differentiating the flow leaving F_i and the flow leaving Q_i, allows us to determine the load and the intensity of traffic crossing F_i. We denote here the probability that the forwarding queue F_i is non-empty by π_i. Similarly, we denote the probability that a packet of the path $R_{s,d}$ is chosen at the beginning of a transmission cycle[2] by $\pi_{i,s,d}$. This quantity is exactly the fraction of traffic related to the path $R_{s,d}$ crossing F_i, thus $\pi_i = \sum_{s,d:i\neq s} \pi_{i,s,d}$. Next we analyze each layer separately and show how coupled they are and derive the metrics of interest.

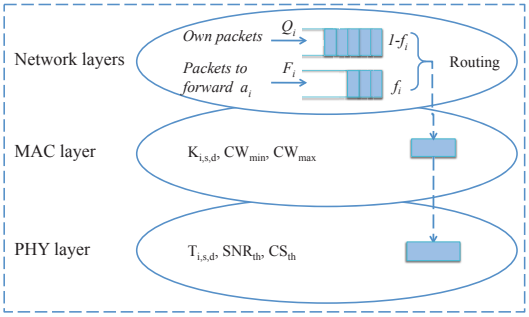

Figure 1. Interaction between NET, MAC and PHY layers.

Attempting the channel begins by choosing the queue from which a packet must be selected. Then, this packet is moved from the corresponding queue at the network layer to the MAC layer where it will be transmitted according to the IEEE 802.11 DCF protocol. In this manner, when a packet is in the MAC layer, it is attempted until it is removed from the node.

Accumulative Interference and virtual node : During a communication between a sender node i and a receiver node j in a given path from s to d (where the

[2] A cycle is defined as the number of slots needed to transmit a single packet until its success or drop. It is formed by the four channel events seen by a sender. For instance : idle slots, busy slots, transmissions with collisions and/or a success.

source node of a connection is s and the destination node is d), the node i transmits to j with a power $T_{i,s,d}$. The received power on j can be related to the transmitted one by the propagation relation $T_{i,s,d} \cdot h_{i,j}$, where $h_{i,j}$ is the channel gain experienced by j on the link (i, j). In order to decode the received signal correctly, $T_{i,s,d} \cdot h_{i,j}$ should exceeds the receiver sensitivity denoted by RX_{th}, i.e., $T_{i,s,d} \cdot h_{i,j} \geq RX_{th}$. Under symmetry assumption and no accumulative effect of concurrent transmissions, the carrier sense range forms a perfect circle with radius r_1. Even when considering accumulative interference, the carrier sense can be reasonably approached by a circle with radius $r_2 \geq r_1$.

Definition 1. *The group $\mathcal{Z}$, composed of nodes that cannot be heard individually by a sender i but their accumulative signal may jam the signal of interest, is called a* ***virtual node****. This way, the virtual node $\mathcal{Z}$ is equivalent to a* ***fictive node*** *being in the carrier sense range of sender i.*

We can then formulate the carrier sense set of a node i by the following expression

$$CS_i = \left\{ \mathcal{Z} : \forall s, d, k' \in \mathcal{Z}, \begin{array}{l} \sum\limits_{k \in \mathcal{Z}} T_{k,s,d} \cdot h_{k,i} \geq CS_{th} \\ \\ \sum\limits_{k \in \mathcal{Z} \setminus k'} T_{k,s,d} \cdot h_{k,i} < CS_{th} \end{array} \right\}, \quad (1)$$

where CS_{th} is the carrier sense threshold. One can see CS_i as the set of virtual nodes that may be heard by sender i when it is sensing the channel in order to transmit on the path $R_{s,d}$. In other words, CS_i is the set of all real nodes (if they are neighbors of i) and virtual nodes (due to accumulative interferences) that may interfere with node i. Now, we define $H_{i,s,d}$ as the set of nodes that may sense the channel busy when node i is transmitting on the path $R_{s,d}$. Then

$$H_{i,s,d} = \{k : T_{i,s,d} \cdot h_{i,k} \geq CS_{th}, \forall s, d\}. \quad (2)$$

For sake of clarity, we are restricted in our formulation to the case of single transmission power. However, our model can be straightforward used for studying power control from nodes individual point of views. An interesting feature is that when the transmission power level is the same for all nodes and accumulative interferences are neglected, $CS_i = H_{i,s,d}$. The receiver $j_{i,s,d}$ can correctly decode the signal from sender node i if the Signal to Interference Ratio (SIR) exceeds a certain threshold SIR_{th}. Let the thermal noise variance, experienced on the path $R_{s,d}$, be denoted by $N_{i,s,d}$, then

$$SIR_{j_{i,s,d}} = \frac{T_{i,s,d} \cdot h_{i,j}}{\sum\limits_{k \neq i} T_{k,s',d'} \cdot h_{k,j} + N_{i,s,d}} \geq SIR_{th}, \ \forall s, d, s', d'. \quad (3)$$

We define now the interference set of a receiver $j_{i,s,d}$ on a path $R_{s,d}$, denoted by $\mathcal{T}_{j_{i,s,d}}$, as the collection of its virtual nodes, i.e., all combination of nodes whose accumulative signal may cause collisions at $j_{i,s,d}$. For instance, the virtual node $\mathcal{Z}$ is in the interference set of node $j_{i,s,d}$ iff the received signal from node i is completely jammed when nodes in $\mathcal{Z}$ are transmitting all together. The interference set of node j is then written as

$$\mathcal{T}_{j_{i,s,d}} = \left\{ \mathcal{Z} : \begin{array}{l} \frac{T_{i,s,d} \cdot h_{i,j}}{\sum\limits_{z \in \mathcal{Z}} T_{z,s',d'} \cdot h_{z,j} + N_{i,s,d}} < SIR_{th}, \\ \\ \frac{T_{i,s,d} \cdot h_{i,j}}{\sum\limits_{z \in \mathcal{Z} \setminus z'} T_{z,s',d'} \cdot h_{z,j} + N_{i,s,d}} \geq SIR_{th}, \\ \\ \forall z', s', d', z' \neq i, s' \neq s, \ d' \neq d. \end{array} \right\} \quad (4)$$

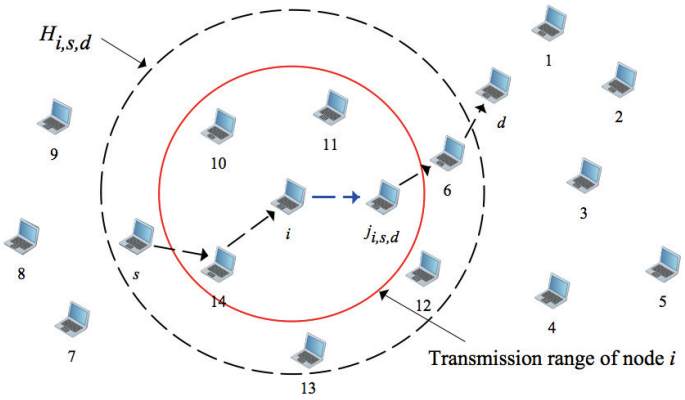

Figure 2. The plot shows the transmission range of node i and the set of real nodes $H_{i,s,d}$ that can hear i when transmitting to node $j_{i,s,d}$. The carrier sense CS_i of node i and the interference set $\mathcal{T}_{j_{i,s,d}}$ are not plotted because they depend on transmit powers of all nodes in the network as well as the topology and scale of the network. For instance $H_{i,s,d} = \{\{s\}, \{j_{i,s,d}\}, \{6\}, \{10\}, \{11\}, \{12\}, \{13\}, \{14\}, \{7, 8, 9\}, \{d, 4\}, \{1, 5, 7, 8\}, \cdots\}$

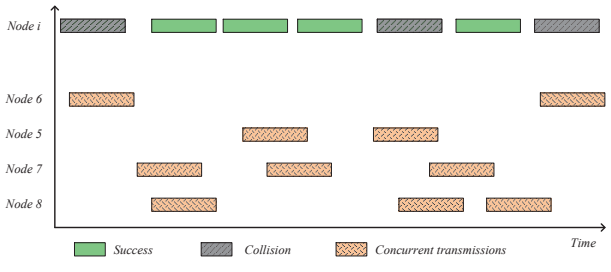

Figure 3. Effect of accumulative interferences on transmission of node i to node j

Fig. 2 shows explicitly two different areas that need to be considered when a couple of nodes

are communicating. Here, we distinguish (i) the transmission area where two nodes can send and receive packets mutually, (ii) the set of nodes that may hear ongoing transmissions of node i, and (iii) implicitly the carrier sense area where two nodes may hear each other but cannot decode the transmitted data. In Fig. 3, we have situated the communication of i and j on the path $R_{s,d}$. Thus, we can integrate the impact of the routing in the model. Fig. 3 illustrates the effect of accumulative interference on the transmission cycles of node i. For illustrative purpose, we consider the following virtual nodes : {6} and {5, 7, 8}. Node 6 is a neighbor of receiver j which causes collision whenever they both (nodes i and 6) are transmitting simultaneously. Whereas a failure may only occur when virtual nodes {5, 7, 8} are all transmitting altogether with sender i.

Each node uses the IEEE 802.11 DCF to access the channel and each one can use different back-off parameters. Let $K_{i,s,d}$ be the maximum number of transmissions allowed by a node i per packet on the path $R_{s,d}$. Then after $K_{i,s,d}$ transmissions the packet is dropped. Also let p_i be the back-off multiplier of a given node i. The maximum stage number of node i is obtained from $W_{m,i} = p_i^{m_i} W_{0,i}$, where $W_{m,i}$ and $W_{0,i}$ are, respectively, the maximum and initial contention window for node i. If $K_{i,s,d} < m_i$ then m_i takes the value of $K_{i,s,d}$, otherwise $m_i = log_{p_i}\left(\frac{W_{m,i}}{W_{0,i}}\right)$. Using a contention window $W_{k,i}$ for stage k of node i, the average back-off time for this stage is $b_{k,i}$. Remark that the back-off parameters of different nodes may be different. Then, the system of nodes are nonhomogeneous as defined by [11].

We consider the modeling problem of the IEEE 802.11 using the perspective of a sender which consists on the channel activity sensed by a sender, or on the state (success or collision) of its transmitted packet. This will facilitate the problem in the ad hoc environment where nodes have an asymmetric vision of the channel. We start by defining the notion of a virtual time slot and channel activity, then we write the expression of the attempt probability for the asymmetric topology. Consider that time is slotted with a physical slot duration τ. Nodes transmit in the beginning of each slot and the transmission duration depends on the type of the transmitted packet. A data packet has a fixed length and takes *Payload* (integer) slots to be transmitted (it includes the header transmission time). While an acknowledgment packet spends *ACK* slots. In our model we consider the two-way handshaking scheme, but it is easily extended to the four-way handshaking scheme. On one hand, a sender node before transmitting would see the channel either busy or idle. On the other hand, its transmitted packet may encounter a success or a collision. These four states define all the possibilities that a sender may observe. Therefore, the average time spent in a given state (seen by this sender) will be referred as the virtual slot of this sender. A remarkable feature here is that this virtual time would depend on the receiver, i.e., on the path where the packet is transmitted. In fact, the success or the collision of the transmitted packet is itself a function of the actual receiver interference state. For that, we denote by $\Delta_{i,s,d}$ the virtual slot seen by node i on the path $R_{s,d}$ that we will derive later on. Considering any asymmetric topology, we will always note the metrics functions of the path chosen for transmission. We recall that when we mention the node $j_{i,s,d}$, it will be clear that this is the receiver of node i on the path $R_{s,d}$.

In the steady-state and such as [5], we use the key assumption which states that at each transmission attempt, and regardless of the number of retransmissions suffered, each packet collides with constant and independent probability. However, collisions may depend only on the receiver channel state. For that we denote by $\gamma_{i,s,d}$ the probability that a transmission of a packet of relay i on the path $R_{s,d}$ fails due to a corruption of either the data or of its acknowledgment. Thus, $(1 - \gamma_{i,s,d})$ is the probability of success on the path $R_{s,d}$. Henceforth, the attempt probability seen by a sender also depends on the receiver, and the well known formula of [5] can be used in the ad hoc network as confirmed in [16]. However, in the asymmetric network the attempt probability $(P_{i,s,d})$ (in a virtual slot) for a node i will be different for each path $R_{s,d}$ and can be written as in [8]:

$$P_{i,s,d} = \frac{1 + \gamma_{i,s,d} + \gamma_{i,s,d}^2 + \cdots + \gamma_{i,s,d}^{K_{i,s,d}-1}}{b_{0,i} + \gamma_{i,s,d} b_{1,i} + \gamma_{i,s,d}^2 b_{2,i} + \cdots + \gamma_{i,s,d}^{K_{i,s,d}-1} b_{K_{i,s,d}-1,i}}, \quad (5)$$

where $b_{k,i} = (p_i^k W_{0,i} - 1)/2$. On average, a node i will attempt the channel (for any path $R_{s,d}$) with a probability P_i which mainly depends on the traffic and the routing table (here, it is maintained by OLSR protocol). Then

$$P_i = \sum_{s,d:i\in R_{s,d}} \pi_{i,s,d} f_i P_{i,s,d} + \sum_d (1 - \pi_i f_i) p_{i,d} P_{i,i,d}. \quad (6)$$

Similarly, the average virtual slot seen by node i is written as

$$\Delta_i = \sum_{s,d:i\in R_{s,d}} \pi_{i,s,d} f_i \Delta_{i,s,d} + \sum_d (1 - \pi_i f_i) p_{i,d} \Delta_{i,i,d}. \quad (7)$$

Remark 1. The *attempt probability (or attempt rate) must be differentiated from the transmission probability. This refers to the probability that a node transmits on* any *slot. Therefore, the transmission probability, if found, can characterize the channel allocation per node. In WLAN, it is sufficient to analyze the back-off rate to determine the channel allocation rate.*

Note that $1-\pi_i f_i$ is the probability to find a packet from Q_i in the MAC layer. It seems important to note that the attempt probability represents the back-off expiration rate. It is the transmission probability in an idle slot (only when the channel is sensed idle). For that, it is convenient to work with MAC protocols that are defined by only an attempt probability, this kind of definition may englobe both slotted Aloha and CSMA type protocols including IEEE 802.11. The problem in ad hoc is that nodes have not the same channel vision (or different back-off parameters) and then the attempt probability may not always describe the real channel access. In [11], the problem of short term unfairness was studied in the context of a WLAN.

Collision probability and virtual slot expressions: The collision probability of a packet occurs when either the data or the acknowledgment experiences a collision. If we denote by $\gamma^D_{i,s,d}$ and $\gamma^A_{j_{i,s,d},s,d}$, respectively, the collision probability of a data packet and its acknowledgement, then we have

$$\gamma_{i,s,d} = 1-\left(1-\gamma^D_{i,s,d}\right)\left(1-\gamma^A_{j_{i,s,d},s,d}\right), \tag{8}$$

The attempt probability of a virtual node $\mathcal{Z}$ is defined by $P_{\mathcal{Z}} = \prod_{z\in\mathcal{Z}} P_z$. Therefore, the virtual slot of a virtual node $\Delta_{\mathcal{Z}}$ can be reasonably estimated using the minimum virtual slot among all nodes in $\mathcal{Z}$, i.e., $\Delta_{\mathcal{Z}} = \min_{j\in\mathcal{Z}} \Delta_j$. Thus the probability that transmitted data collides with other concurrent transmissions can be written as

$$\gamma^D_{i,s,d} = 1-\prod_{k\in H_{i,s,d}\cap\mathcal{T}_{j_{i,s,d}}}(1-P_k)\left(1-\sum_{\mathcal{Z}\in\mathcal{T}_{j_{i,s,d}}\setminus H_{i,s,d}} P_{\mathcal{Z}}^{\frac{Payload}{\Delta_{\mathcal{Z}}}}\right). \tag{9}$$

Indeed, nodes in area $H_{i,s,d}\cap\mathcal{T}_{j_{i,s,d}}$ must be silent at the beginning of node i transmission. While nodes in $\mathcal{T}_{j_{i,s,d}}\setminus H_{i,s,d}$ are hidden to i (they constitute the virtual nodes of i) and needs to be silent during all the data transmission time which is a vulnerable time. The $\frac{Payload}{\Delta_j}$ is the normalized vulnerable time. After the beginning of data transmission, nodes in $H_{i,s,d}$ will defer their transmission to $EIFS$ (Extended Inter-Frame Space) duration, which would insure the good reception of the acknowledgment. In practice, acknowledgement are small packets and less vulnerable to collision, for that it is plausible to consider $\gamma^A_{j_{i,s,d},s,d}\simeq 0$. Then, we can write $\gamma_{i,s,d} = \gamma^D_{i,s,d}$.

Considering the previously defined four states and from the view of node i, the network stays in a single state a duration equal to $\Delta_{i,s,d}$. It is given by

$$\Delta_{i,s,d} = P^{succ}_{i,s,d}.T_{succ} + P^{col}_{i,s,d}.T_{col} + P^{idle}_i.T_{idle} + P^{busy}_i.T_{busy}, \tag{10}$$

where $T_{succ} = Payload + ACK + SIFS + DIFS$, $T_{col} = Payload + ACK + DIFS$, $T_{idle} = \tau$, $T_{busy} = Payload + DIFS$, $P^{succ}_{i,s,d} = P_{i,s,d}(1-\gamma_{i,s,d})$, $P^{col}_{i,s,d} = P_{i,s,d}\gamma_{i,s,d}$, $P^{idle}_i = \prod_{\mathcal{Z}\in CS_i\cup\{i\}}(1-P_{\mathcal{Z}})$, and $P^{busy}_i = (1-P_i)\sum_{\mathcal{Z}\in CS_i} P_{\mathcal{Z}}$.

Finally, let us denote the equations (5), (6), (8) and (10) by *system I*. Normally, it is sufficient to solve the *system I* to derive the fixed points of each node. However, by introducing the traffic metric in equations (6) and (7), these equations cannot be solved without knowing the $\pi_{i,s,d}$ which is defined as the traffic intensity for each path $R_{s,d}$ crossing node i. Therefore, in Section 3, we proceed in writing the rate balance equations at each node, from which $\pi_{i,s,d}$ can be derived as a function of P_j and $\gamma_{j,s,d}$, for all j. These rate balance equations give the traffic intensity. The problem resides in the complexity of the systems and in the computational issue.

3. End-to-end throughput and traffic intensity system

We are interested in this section to derive the end-to-end throughput per connection, function of different layer parameters, including the IEEE 802.11 parameters. It is clear that the average performance of the system is hardly related to the interaction PHY/MAC/NETWORK. We focus on the traffic crossing the forwarding queues, which may be an issue on the buffers' stability. Now, if the arrival and the service rates of a queue are stationary then, from Loynes'ĂŹs theorem, the queue is stable if the arrival rate is less then the service rate. Usually, the stability region is defined to be the closure of the set of all arrival rates vectors such that the network can be stabilized. Hence if the queue F_i is stable, then the departure rate of packets from Fi is equal to the arrival rate into it. This is a simple definition of balance rate in the stability region. We are going to derive this equation for each node i and each connection $R_{s,d}$. The system of these equations, for all i and $R_{s,d}$, will form the traffic intensity system, it will be referred as *system II*. In sum, we are writing a system that determines $\pi_{i,s,d}$ for all i and $R_{s,d}$. For that, we first derive the average length of a transmission cycle per packet C_i at node i. A cycle length on the path $R_{s,d}$ is formed by the attempt slots that do not lead to a channel access, to a transmission and retransmissions of the same packet until a success or a drop. A cycle may contain idle periods, busy periods, collision periods or/and at most one successful transmission period. Let the random variable (r.v.) X_i (resp. Y_i, Z_i and V_i) be the number of idle period (resp. the number of busy period, the number of collision period and the number successful period) in a cycle on the path $R_{s,d}$. Hence the

average length in slots of this cycle is given by

$$\begin{aligned}\hat{C}_{i,s,d} &= \sum_{k=1}^{K_{i,s,d}-1}\sum_{l=0}^{\infty}\sum_{h=0}^{\infty}\binom{l+h+k}{l}\binom{h+k}{h} \\ &\times (l.T_{idle}+h.T_{busy}+k.T_{col}+T_{succ}).Pr_{l,h,k,1} \\ &+ \binom{l+h+K_{i,s,d}-1}{l}\binom{h+K_{i,s,d}-1}{h} \\ &\times (l.T_{idle}+h.T_{busy}+K_{i,s,d}.T_{col}).Pr_{l,h,K,0}, \quad (11)\end{aligned}$$

where $Pr_{l,h,k,j} = (P_i^{idle})^l (P_i^{busy})^h (P_{i,s,d}^{col})^k (P_{i,s,d}^{succ})^j$. When a node transmits to several paths, we need to know the average cycle length. Hence, the average cycle of a node is given by

$$C_i = \sum_{s,d:i\in R_{s,d}} \pi_{i,s,d} f_i \hat{C}_{i,s,d} + \sum_d (1-\pi_i f_i) p_{i,d} \hat{C}_{i,i,d} \quad (12)$$

To write the departure rate from F_i as well as the arrival rate into the queue, let us first consider the following counters :

- $C_{t,i}$ is the number of cycle of the node i till the t^{th} slot, where t slots means t physical slots and it is equivalent to $t.\delta$ seconds with $\delta = 20\mu s$ in the IEEE 802.11.
- $C_{t,i}^F$ (resp. $C_{t,i}^Q$) is the number of all *forwarding cycles* (resp. *source cycles*) of the node i till the t^{th} slot.
- $C_{t,i,s,d}^F$ (resp. $C_{t,i,s,d}^Q$) is the number of *forwarding cycles* (resp. *source cycles*) corresponding to the path $R_{s,d}$ of the node i till the t^{th} slot.
- $T_{t,i,s,d}$ is the number of times we found at the first slot of a cycle and at the first position in the queue F_i a packet for the path $R_{s,d}$ of the node i till the t^{th} slot.
- $I_{t,i,s,d}$ is the number of cycles corresponding to the path $R_{s,d}$ of the node i, where a cycle is ended by a success of the transmitted packet till the t^{th} slot.
- $A_{t,i,s,d}$ is the number of arrival packets to node i on the path $R_{s,d}$.

Departure rate : The departure rate from F_i is the probability that a packet is removed from node i (forwarding queue) by either a successful transmission or a drop after successive $K_{i,s,d}$ failures. The departure rate regarding only the packets sent on the path $R_{s,d}$ is denoted by $d_{i,s,d}$. Formally, for any node i, s and d such that $p_{s,d} > 0$ and $i \in R_{s,d}$, the long term departure rate of packets from node i on the route from s to d is given by the following theorem:

Theorem 1. *The long term departure rate from node i related to path $R_{s,d}$ is given by*

$$d_{i,s,d} = \frac{f_i \pi_{i,s,d}}{C_i}. \quad (13)$$

Proof. The long term departure rate of packets from node i on the route from s to d is

$$\begin{aligned} d_{i,s,d} &= \lim_{t\to\infty} \frac{C_{t,i,s,d}^F}{t} \\ &= \lim_{t\to\infty} \frac{T_{t,i,s,d}}{C_{t,i}} \cdot \frac{C_{t,i,s,d}^F}{T_{t,i,s,d}} \cdot \frac{C_{t,i}}{t}. \quad (14)\end{aligned}$$

- $\lim_{t\to\infty} \frac{T_{t,i,s,d}}{C_{t,i}}$ is the probability that F_i carries a packet to the path $R_{s,d}$ at the beginning of each cycle. Therefore $\lim_{t\to\infty} \frac{T_{t,i,s,d}}{C_{t,i}} = \pi_{i,s,d}$.
- $\lim_{t\to\infty} \frac{C_{t,i,s,d}^F}{T_{t,i,s,d}}$ is exactly the probability that a packet is chosen from F_i to be sent when F_i carried a packet to the path $R_{s,d}$ in the first position and in the beginning of a forwarding cycle. Therefore, $\lim_{t\to\infty} \frac{C_{t,i,s,d}^F}{T_{t,i,s,d}} = f_i$.
- $\lim_{t\to\infty} \frac{t}{C_{t,i}}$ is the average length in slots of a cycle of the node i. Moreover, we have

$$d_{i,s',d'} = \frac{\pi_{i,s',d'} f_i}{\sum_{s,d:i\in R_{s,d}} \pi_{i,s,d} f_i \hat{C}_{i,s,d} + \sum_d (1-\pi_i f_i) p_{i,d} \hat{C}_{i,i,d}}. \quad (15)$$

Hence from (12), it is easy to derive the total departure rate d_i on all paths:

$$d_i = \sum_{s',d':i\in R_{s',d'}} d_{i,s',d'} = \frac{\pi_i f_i}{C_i}. \quad (16)$$

□

Arrival rate and end-to-end throughput : The probability that a packet arrives to the queue F_i of the node i is also called the arrival rate, we denote it by a_i. When this rate concerns only packets sent on the path $R_{s,d}$, we denote it by $a_{i,s,d}$. Formally, for any nodes i, s and d such that $p_{s,d} > 0$ and $i \in R_{s,d}$, the long term arrival rate of packets into F_i for $R_{s,d}$ is provided by the following theorem

Theorem 2. *The long term arrival rate into node i forwarding queue, related to path $R_{s,d}$, is given by*

$$a_{i,s,d} = (1-\pi_s f_s) \cdot \frac{p_{s,d}}{C_s} \cdot \prod_{k\in R_{s,i}\cup s} \left(1-\gamma_{k,s,d}^{K_{k,s,d}}\right). \quad (17)$$

Proof. The long term arrival rate of packets into F_i for $R_{s,d}$ is

$$\begin{aligned} a_{i,s,d} &= \lim_{t\to\infty} \frac{A_{t,i,s,d}}{t} \\ &= \lim_{t\to\infty} \frac{C^Q_{t,s}}{C_{t,s}} \cdot \frac{C^Q_{t,s,s,d}}{C^Q_{t,s}} \cdot \frac{C_{t,s}}{t} \cdot \frac{I_{t,s,s,d}}{C^Q_{t,s,s,d}} \cdot \frac{A_{t,i,s,d}}{I_{t,s,s,d}}. \quad (18) \end{aligned}$$

- $\lim_{t\to\infty} \frac{C^Q_{t,s}}{C_{t,s}} = 1 - \frac{C^F_{t,s}}{C_{t,s}} = 1 - \pi_s f_s$ is exactly the probability to get a source cycle, i.e., to send a packet from the queue Q_s.
- $\lim_{t\to\infty} \frac{C^Q_{t,s,s,d}}{C^Q_{t,s}}$ is the probability to choose the path $R_{s,d}$ to send a packet from Q_s. Therefore, $\lim_{t\to\infty} \frac{C^Q_{t,s,s,d}}{C^Q_{t,s}} = p_{s,d}$.
- $\lim_{t\to\infty} \frac{C_{t,s}}{t} = \frac{1}{C_s}$.
- $\lim_{t\to\infty} \frac{I_{t,s,s,d}}{C^Q_{t,s,s,d}}$ is the probability that a source cycle on the path $R_{s,d}$ ends with a success, i.e., the packet sent from Q_s is received on the queue $F_{j_{s,s,d}}$. Therefore, $\lim_{t\to\infty} \frac{I_{t,s,s,d}}{C^Q_{t,s,s,d}} = 1 - \gamma^{K_{s,s,d}}_{s,s,d}$.
- $\lim_{t\to\infty} \frac{A_{t,i,s,d}}{I_{t,s,s,d}}$ is the probability that a packet received on the node $j_{s,s,d}$ is also received on the queue F_i of the node i. For that, this packet needs to be received by all the nodes in the set $R_{s,i} \cup s$. Therefore, $\lim_{t\to\infty} \frac{A_{t,i,s,d}}{I_{t,s,s,d}} = \prod_{k\in R_{s,i}\cup s} \left(1 - \gamma^{K_{k,s,d}}_{k,s,d}\right)$.

Consequently, the result of the theorem holds. □

End-to-end throughput : The global arrival rate at F_i is $a_i = \sum_{s,d:i\in R_{s,d}} a_{i,s,d}$. Remark that when the node i is the final destination of a path $R_{s,d}$, then $a_{d,s,d}$ represents the end-to-end average throughput of a connection from s to d. Practically, $a_{d,s,d}$ is the number of delivered (to destination) packet per slot. Let ρ be the bit rate in bits/s of the wireless network. Therefore, the throughput in bits/s can be written as follows:

$$thp_{s,d} = a_{d,s,d} \cdot Payload \cdot \rho. \quad (19)$$

Rate balance equations/traffic intensity system : Finally, in the steady state if all the queues in the network are stable, then for each i, s and d such that $i \in R_{s,d}$ we get $d_{i,s,d} = a_{i,s,d}$, which is the rate balance equation on the path $R_{s,d}$. For all i, s and d we get the traffic intensity system: *system II*. When we sum both the sides of this last system, we get the global rate balance equation: $d_i = a_i$.
Let $y_i = 1 - \pi_i f_i$ and $z_{i,s,d} = \pi_{i,s,d} f_i$. Thus $y_i = 1 - \sum_{s,d:i\in R_{s,d}} z_{i,s,d}$. Then, the rate balance equation can be written in the following form:

$$\sum_{d:i\in R_{s,d}} z_{i,s,d} = \frac{y_s(\sum_{s',d'} z_{i,s',d'}\hat{C}_{i,s',d'} + \sum_{d''} y_i p_{i,d''}\hat{C}_{i,i,d''})w_{s,i}}{(\sum_{s',d'} z_{s,s',d'}\hat{C}_{s,s',d'} + \sum_{d''} y_s p_{s,d''}\hat{C}_{s,s,d''})}, \quad (20)$$

where $w_{s,i} = \sum_{d:i\in R_{s,d}} p_{s,d} \prod_{k\in R_{s,i}\cup s} \left(1 - \gamma^{K_{k,s,d}}_{k,s,d}\right)$.
An interesting interpretation and application of equation (20) are the following : (i) $z_{i,s,d}$ and y_i (can be considered as the stability region of node i) are independent of the choice of f_i. (ii) For some values of f_i the forwarding queue of node i will be stable. Regarding P_i, we notice that it can be written as $P_i = \sum_{s,d:i\in R_{s,d}} z_{i,s,d} P_{i,s,d} + \sum_d y_i p_{i,d} P_{i,i,d}$. Then it depends on $z_{i,s,d}$ and y_i, but it is not affected by f_i. A similar deduction is also observed for the energy consumed when sensing the channel or transmitting data. Let $E_{i,s,d}$ be the expression of the energy consumed per cycle by each node on the path $R_{s,d}$. Let also E^s_i be the energy consumed per (virtual) slot in sensing the channel, and $E^{tx}_{i,s,d}$ be the energy consumed per transmission of a single packet on the path $R_{s,d}$. Therefore, we can derive $E_{i,s,d}$ from the average cycle length of equation (11) as follows:

$$\begin{aligned} E_{i,s,d} &= \sum_{k=1}^{K_{i,s,d}-1} \sum_{l=0}^{\infty} \sum_{h=0}^{\infty} \binom{l+h+k}{l} \binom{h+k}{h} \\ &\times (l.T_{idle}.E^s_i + h.T_{busy}.E^s_i + k.T_{col}.E^{tx}_{i,s,d} \\ &+ T_{succ}.E^{tx}_{i,s,d}).Pr_{l,h,k,1} \\ &+ \binom{l+h+K_{i,s,d}-1}{l} \binom{h+K_{i,s,d}-1}{h} \\ &\times (l.T_{idle}.E^s_i + h.T_{busy}.E^s_i + K_{i,s,d}.T_{col}.E^{tx}_{i,s,d}).Pr_{l,h,K,0}. \end{aligned}$$

This quantity turns out to be independent of the choice of f_i. Hence, the node can use f_i to improve the expected delay without affecting the energy consumption. Note that the value $\pi_{i,s,d} f_i E^{i,s,d}_r$ represents the energy consumption used by node i to forward packets to path $R_{s,d}$, where $E^{i,s,d}_r$ is the energy spent for transmission of one packet.

Resolving PHY/MAC/NETWORK coupled problems : As have shown previously, the MAC layer systems of fixed points and the Network layer rate balance systems (non linear systems) could not be resolved separately. Moreover, due to dependance on topology, routing and users' behaviors, we cannot show analytically existence of a unique solution of the fixed point systems. However, for several scenarios and network topologies, *system I* and *system II* always provide the same solution as obtained from simulation. We give in algorithm 1 a sketch of the algorithmic way we follow to solve mutually the above systems (including the correlation between layers).

Algorithm 1 : Joint fixed point and rate balance resolution

Require: $\pi^0_{i,s,d} = \epsilon_{i,s,d}$, $\delta_{i,s,d}$: convergence indicator of path $R_{s,d}$

1: **for** each source s, relay i and destination d **do**
2: **while** $\left|\frac{\pi^{t+1}_{i,s,d} - \pi^t_{i,s,d}}{\pi^t_{i,s,d}}\right| \geq \delta_{i,s,d}$ **do**
3: Compute $P_{i,s,d}$ using fixed point such as [8]
4: Update $\gamma_{i,s,d}$ using equation (9)
5: Estimate cycles size using equation (12)
6: Update $\pi^{t+1}_{i,s,d}$ by solving the rate balance system (20) using for example the Gaussian elimination method
7: **end while**
8: **end for**

Special Cases : For sure the *system I* and *system II* are complicated to solve and computational expensive. For that, special cases are important and would facilitate the analysis of the systems and can be useful and easy to use in numerical results. As we have mentioned previously, $P_{i,s,d}$ and $\gamma_{i,s,d}$ need to be found jointly with $\pi_{i,s,d}$. This is due to the traffic asymmetry. Furthermore, the average cycle length C_i is a function of $\pi_{i,s,d}$. This also complicate the calculation of $\pi_{i,s,d}$, when $P_{i,s,d}$ and $\gamma_{i,s,d}$ are given. Therefore, two special cases can be distinguished as follows:

- Uniform traffic distribution and symmetric topology: $\gamma_{i,s,d} \equiv \gamma_i$ and $P_{i,s,d} \equiv P_i$. Also, $C_i \equiv \hat{C}_{i,s,d}$.
- Uniform traffic distribution and asymmetric topology: $\gamma_{i,s,d} \neq \gamma_i$ and $P_{i,s,d} \neq P_i$. Also, $C_i \neq \hat{C}_{i,s,d}$, except the case where the routing at each node chooses the same next hop to route packets for all paths $R_{s,d}$.

In these two cases, the *System I* is independent of $\pi_{i,s,d}$, i.e., *System I* and *system II* are decoupled. Therefore, we can find the attempt and collision probabilities in *System I*, and then calculate the traffic intensity. In addition, the *system II* becomes a linear system that can be solved easily. Therefore, the *system II* can be written as:

$$1 - y_i = \sum_s y_s \bar{w}_{s,i}, \tag{21}$$

where

$$\bar{w}_{s,i} = \sum_{d:i\in R_{s,d}} P_s p_{s,d} \hat{C}_{i,s,d} \prod_{k\in R_{s,i}} \left(1 - \gamma^{K_{k,s,d}}_{k,s,d}\right). \tag{22}$$

Therefore, we can write it in a matrix form:

$$\underline{y}(I + \bar{W}) = \underline{1}, \tag{23}$$

where $\bar{W}$ is an $N \times N$ matrix whose $(s,i)^{th}$ entry is $\bar{w}_{s,i}$ (independent on y_i) and $\underline{y}$ is a $N-$dimensional row vector. In addition, *system I* will be simplified when no hidden nodes are found in the network. This case can happen when the interference area of receivers j is included in the carrier sense area of each sender i, i.e., $I_j \setminus CS_i = \varnothing$. This imply that $\gamma_{i,s,d}$ is independent of the virtual slot $\Delta_{i,s,d}$.

4. Simulation and numerical investigations

We turn in this section to study a typical example of multi-hop ad hoc networks. We consider an asymmetric network formed by 9 nodes and these nodes are identified using integers from 1 to 9 as shown in Fig. 4. We establish 9 connections (or paths) labeled by letters from a to i. Each node is located by its plane Cartesian coordinates expressed in meters. Apart from this, the main parameters are fixed to the following values : $CW_{min} = 32$, $CW_{max} = 1024$, $K_{i,s,d} \equiv K = 4$, $f_i \equiv f = 0.9$ (to insure stability of forwarding queues), $T_{i,s,d} \equiv T = 0.1W$ $(\forall i,s,d)$, $CS_{th} = 0$ dBm, $RX_{th} = 0$ dBm, $SIR_{th} = 10$ dB (target SIR), $\rho = 2$ Mbps (bit rate), $\alpha = 2$ (path loss exponent factor), $c = 6$ dBi (antenna gain), $\delta = 20\mu s$ (physical slot duration), $DISF = 3\delta$ and $SIFS = \delta$.

Model validation : We now present extensive

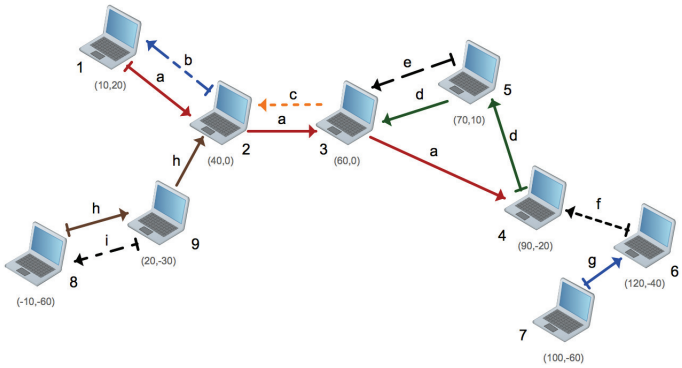

Figure 4. The multi-hop wireless ad hoc network used for simulation and numerical examples.

numerical and simulation results to show the accuracy of our model and study the impact of joint PHY, MAC and NETWORK parameters. For this purpose, a discrete time simulator which implements the IEEE 802.11 DCF, integrating the weighted fair queueing over two buffers discussed before, is used to simulate the former network. Each simulation is realized during 10^6 physical slots, repeated at least 20 times and then averaged to smooth out the fluctuations caused by random number generator of the simulator. We checked the validity of the model by extensively considering different network scenarios and topologies. We depict in Fig. 5 (resp. Fig. 6) the analytic as well as the simulative average load of forwarding queues (resp. average end-to-end delay of considered connections).

Numerical plots show that analytic model match well with the simulative results, in particular under the stability region which is the main applicability region of our model. With some abuse we refer to the interval of forwarding probability that insure a load strictly less than 1 for all queues, as the stability region. The main difference seen between individual loads is mainly due to the topology asymmetry. Based on Fig. 6, we note that our analytic result says that under the stability condition, the end-to-end throughput does not depend on the choice of the WFQ weight, i.e., on the cooperation level or forwarding probability. Therefore, one can judiciously fine-tune the cooperation level value to decrease the delay when the average throughput is kept almost constant. This mechanism may play a crucial role in delay sensitive traffic support over multi-hop networks. Later, we plot the average throughput versus the normalized payload size (the number of slots required to transmit a packet). We conclude from Fig. 7 that an optimal payload size may not exist. Indeed, we note that some specific payload size is providing good performances in term of average throughput over some paths, but may hurt drastically the throughput of other links and then the reachability becomes a real issue. *Setting the payload size to a fixed value over the whole network is, in general, unfair and is not suitable for multi-hop networks*. However fortunately, existence of locally optimal payload size may exist. This way, it depends strongly on the topology and the local node densities, i.e., the number of neighbors, their respective distances with respect to a tagged node and how they are distributed in the network. Fig. 8 shows the variation of average loads of intermediate nodes as a function of the normalized payload. Here, π_i is strictly decreasing for all nodes i. This provides an intuition to limit the forwarding queue load (equivalently the delay) by setting the payload size to a high value. Unfortunately, this is unfair and may hurt some connections with more penalizing environment and bad channel state.

Fig. 9 plots the average throughput experienced by all established connections when varying the minimum contention window CW_{min}. We remark that the throughput behaves in two different ways according to the topology of the multi-hop network. Indeed, when the node density is low, the throughput is maximized for short backlog duration (connections e, g and i). Here, nodes take advantage from local node density and tend to transmit more aggressively, having a relatively low collision probability due to low number of competitors. Whereas for other connections, the optimal contention windows size is different from CW_{min} defined by the IEEE 802.11 DCF standard. We also note that the contention window tends to increase as the node density becomes high. This latter remark is quite intuitive and due to the fact that the competition

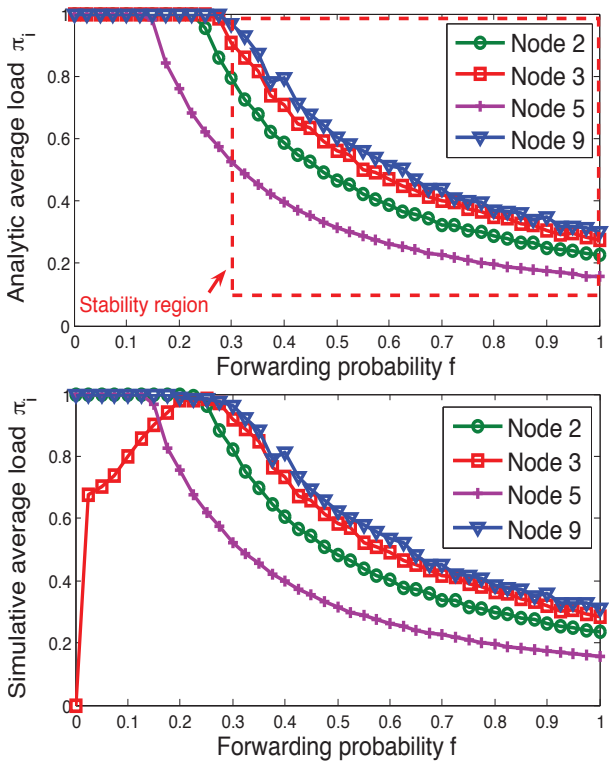

Figure 5. Average forwarding queues load from model versus simulation as function of forwarding probability.

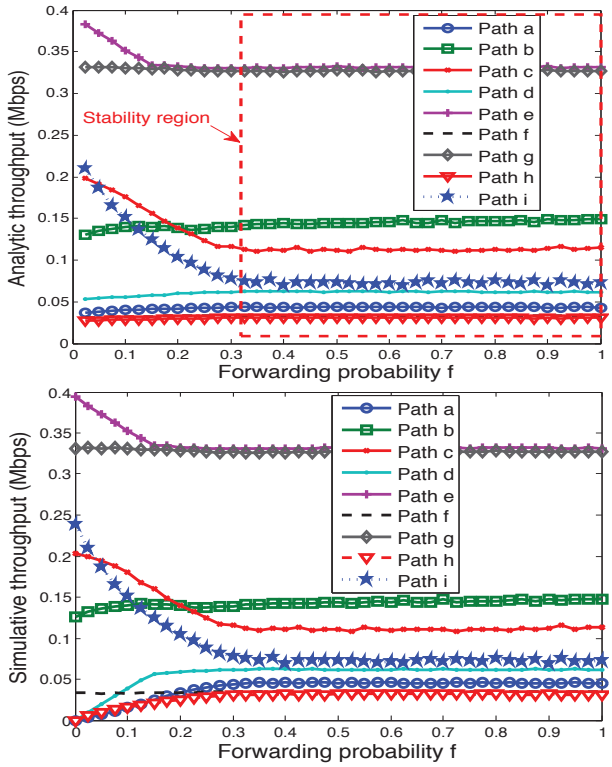

Figure 6. Average end-to-end throughput from model versus simulation as function of forwarding probability.

becomes colossal. In terms of queue load (equivalently delay), it is clear that when the contention window increases it implies the increase of queue load and henceforth tagged node may suffer from huge delay.

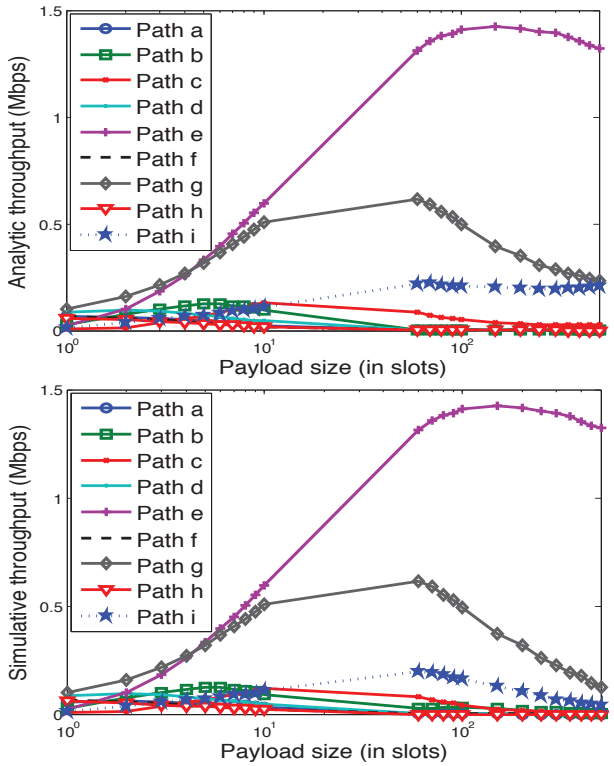

Figure 7. Average end-to-end throughput from model versus simulation when varying the payload size.

Per path power and carrier sense control : We reconsider here the Spanning tree-based algorithm proposed in [9]. *Each node sets its transmission power to a level that allows reaching the farthest neighbor*, i.e., the received power is at least equal to the receiver sensitivity. Consequently, this per path power control may improve the spatial reuse. In order to analyze the impact of carrier sense threshold on network performances, we will vary CS_{th} for some tagged node and fix it to the default value, i.e., $CS_{th} = 0$ dBm. We plot in Fig. 12 the average throughput of all paths when varying the carrier sense threshold of node 3 which is located in a relatively dense subnetwork. We note that the throughput of all connections continues to decrease (in particular connections crossing node 3 or its immediate neighbors) with CS_{th} except connections originated from node 3. Now we analyze the interplay of node 8 (in a low dense subnetwork) carrier sense on network performances. We note that the only negatively impacted connection is connection i originated from node 9 (immediate neighbor of node 8). When carrier sense of node 8 is increasing, it becomes more nose-tolerable which implies a more transmission

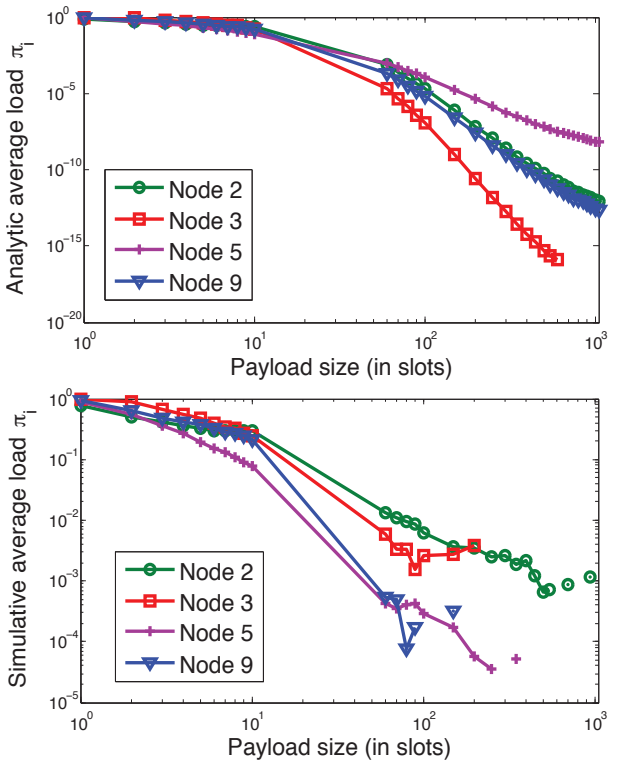

Figure 8. Average load of forwarding queues from model versus simulation when varying the payload size.

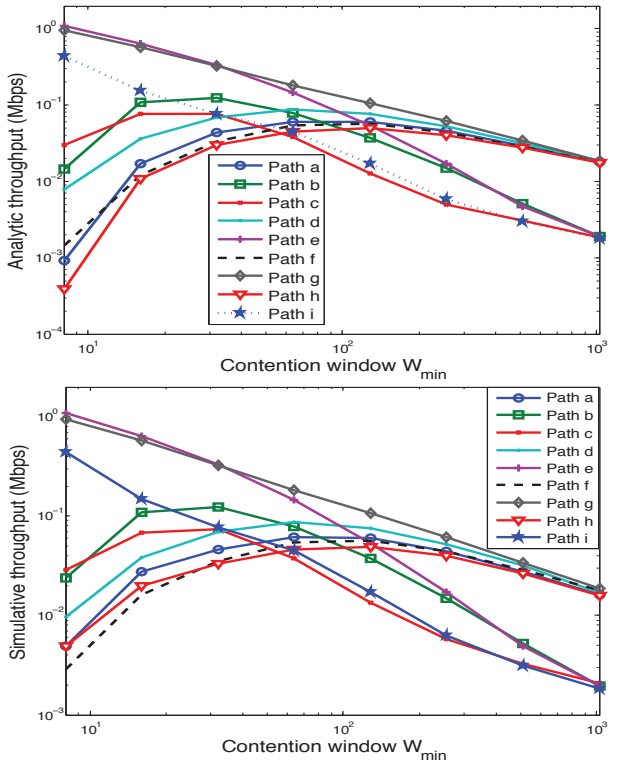

Figure 9. Average end-to-end throughput from model versus simulation when varying the minimum contention window.

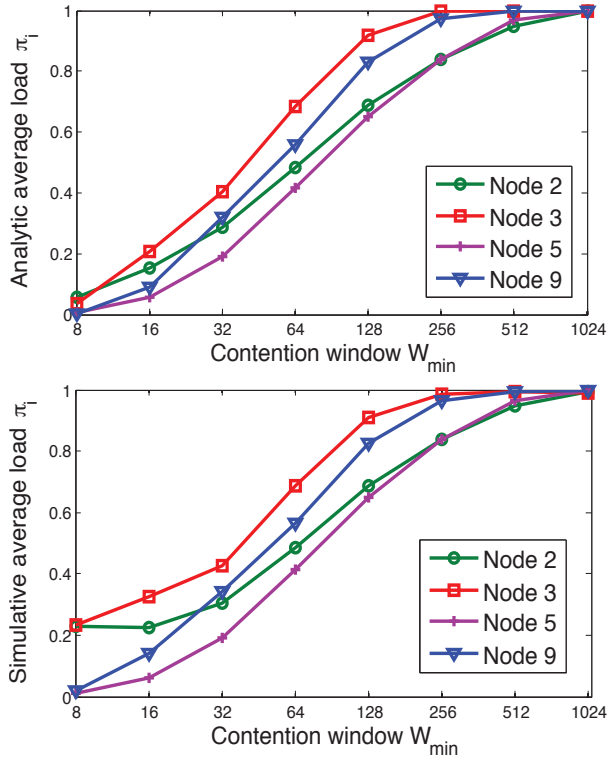

Figure 10. Average load of forwarding queues from model versus simulation when varying the minimum contention window.

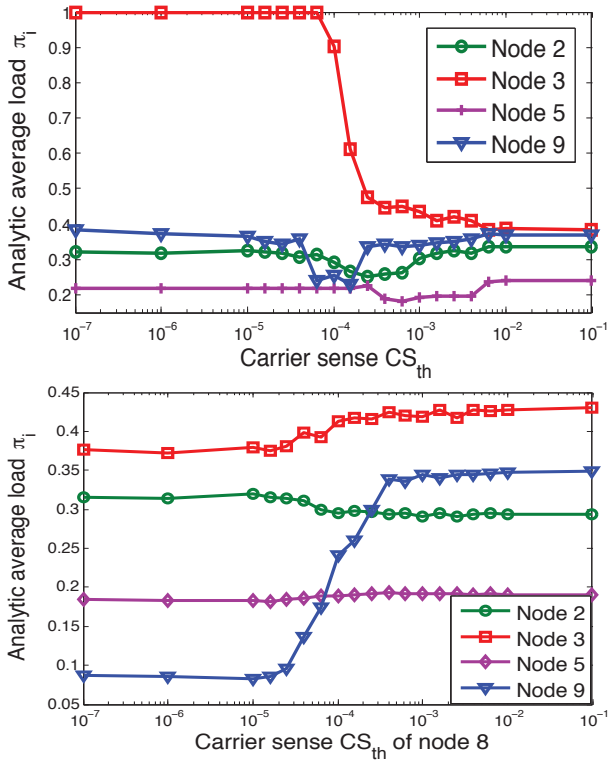

Figure 11. Average load of forwarding queues from model versus simulation for variable carrier sense threshold (in Watt).

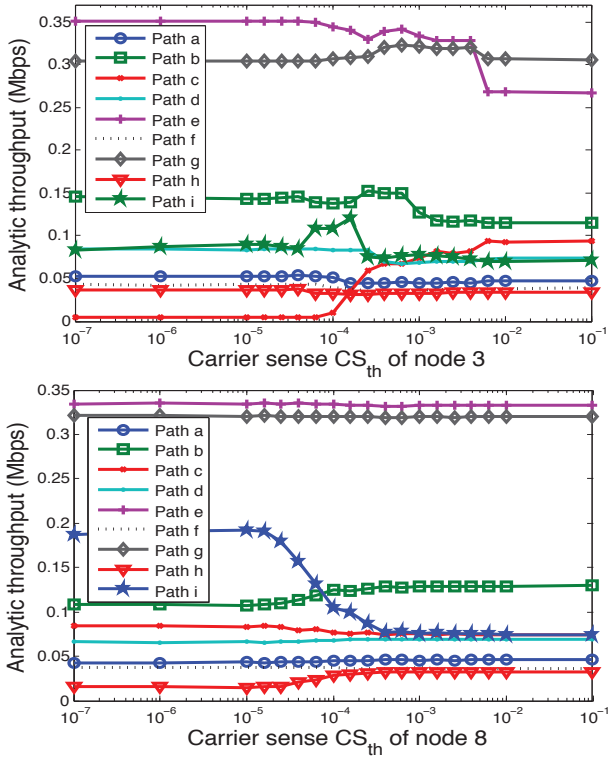

Figure 12. End-to-end throughput from model versus simulation for variable carrier sense threshold (in Watt).

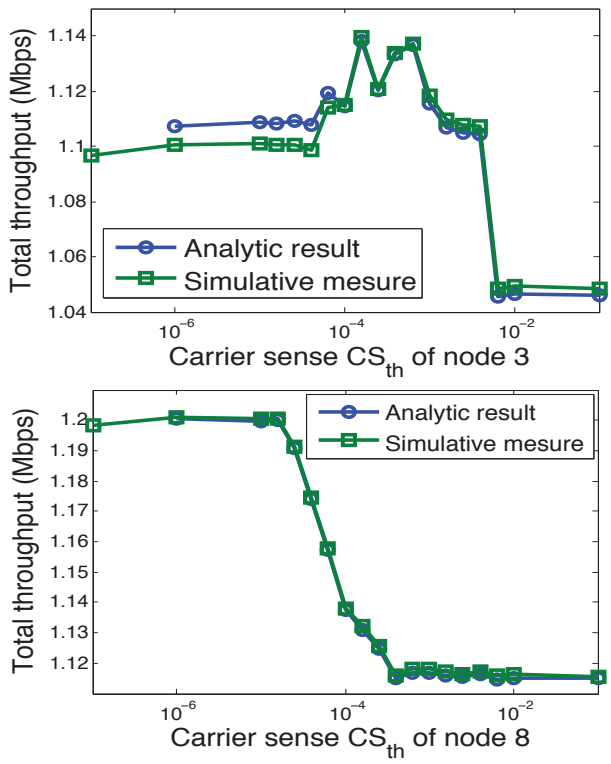

Figure 13. End-to-end throughput from model versus simulation for variable carrier sense threshold (in Watt).

aggressiveness. Which explain the throughput decrease of connection i due to larger backoff duration of node 9 to resolve collision. Thus connections crossing neighbors of node 9 take advantage from the low attempt rate of node 9 to improve their throughput, for instance connections a, b and h.

Aggregate throughput : In terms of total capacity and depending on the local node density, the CSC may increase the network throughput. Indeed, when a node in a dense zone fine-tunes its carrier sense threshold, we note existence of a region where the total capacity is maximized. This region correspond to a CS_{th} interval where a tagged node benefits from relatively high throughput and other nodes do not suffer much from this. Whereas, it seems that allowing nodes in low dense parts of the network may cause a throughput decrease due to selfishness of tagged nodes. To sum up, we can say that on one hand, a higher carrier sense threshold encourages more concurrent transmissions but at the cost of more collisions. On the other hand, a lower carrier sense threshold reduces the collision probability but it requires a larger spatial footprint and prevents simultaneous transmissions from occurring, which may result in limiting the system throughput.

Discussion : In contrast to classical systems where all users communicate with an access point and have, in general, the same channel/environment, in ad hoc networks, the main difference is the variable topology and the asymmetric view. A judicious and punctual solution is to auto-configure parameters of the PHY/MAC/NETWORK by the node itself. However unfortunately, this may result in a performance collapse due to users selfishness (similar to prisoners dilemma in game theory). We also suggest to run a MAC/PHY cross-layer control where each node is increasing the transmit power whenever a retransmission is needed. Unfortunately, this power control seems to be unfair since the benefit is strongly depending on the topology. Due to asymmetry, many nodes take benefit from this policy but others may hardly suffer from it. To sum up, under topology asymmetry, the problem is not how to choose parameters such as the network may operate in an optimal way; but the problem is how to define a cooperation level and a trade-off between end-to-end throughput and delay.

Analyzing Fig. 14 where the behavior of the total capacity is depicted as a function of nodes intrinsic parameters (f_i, $Payload_i$ and CW_i), we note that the capacity is maximal when a node behaves selfishly, i.e., $f = 0$. It was shown in our earlier work [7] that a maximum throughput is achieved in the shortest path. A high amount of traffic in the topology of Fig. 4 is issued from one hop paths, which explains the continuous decrease of the capacity with cooperation level f. However, the cooperation is crucial to maintain the network connectivity. In view of a game theory and

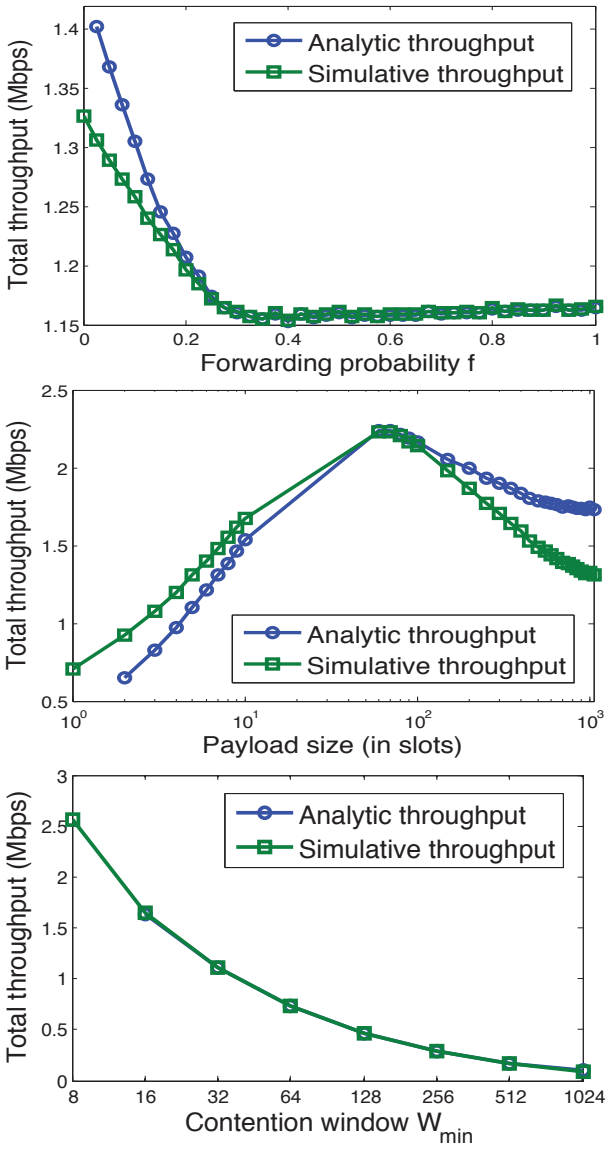

Figure 14. Average cycle size from model versus simulation under different parameters variation.

under node rationality assumption, if a node refuses to forward packets of neighboring nodes then the other may behave similarly. As a result the total capacity may fall down drastically and delay may go to infinity (very large waiting time in intermediate buffers). A challenging but promising concept is then to enable an autonomous location and environment-aware feature. Here, each node may sense the channel, learn the channel state/network topology, decide the best setup, adapt its parameters and reconfigure them till desired QoS is achieved. Nodes can then share their respective information for better environment awareness and less signaling traffic.

5. Conclusion

In multi-hop ad hoc network, a stack of protocols would interact with each other to accomplish a successful packet transfer. In this context, we have developed a cross-layered model built on the IEEE 802.11e EDCF standard. We studied the effect of forwarding on end-to-end performances for saturated networks. We have discovered that the modeling of the IEEE 802.11 in this context is not yet mature in the literature and to the best of our knowledge, there is no study done which considers jointly the PHY/MAC/NETWORK interaction in a non-uniform traffic and a general network topology. This has led us to build a general framework using the perspective of individual senders. The attempt and collision probabilities are now functions of the traffic intensity, on topology and on routing decision. The fixed point *system I* is indeed related to the traffic intensity *system II*.

This paper opens many interesting directions to study in future such as power control and delay-based admission control with guaranteed throughput. Moreover, we will deal with the issue of cooperation between nodes in a game theoretical perspective. In addition, our proposal could be easily extended for very high data rate IEEE 802.11n or the future standard IEEE 802.11ac.

References

[1] B. Alawieh, C. Assi, H.T. and Mouftah. Investigation of power-aware IEEE 802.11 performance in multi-hop ad hoc networks. In Proceedings of International Conference on Mobile Ad-hoc and Sensor Networks (MSN), pages 409-420, 2007.

[2] Alizadeh-Shabdiz, F., and Subramaniam, S.: Analytical models for single-hop and multi-hop ad hoc networks. Mob. Netw. Appl., 11(1):75-90, 2006.

[3] Baras, J. S., Tabatabaee, V., Papageorgiou, G., and Rentz, N.: Modelling and optimization for multi-hop wireless networks using fixed point and automatic differentiation. In WiOpt 2008, 6th IEEE International Symposium on Modeling and Optimization in Mobile, Ad Hoc, and Wireless Networks, March 31 - April 4 2008.

[4] Y. Barowski S. Biaz and P. Agrawal. Towards the performance analysis of IEEE 802.11 in multi-hop ad-hoc networks. In Proceedings of IEEE Wireless Communications and Networking Conference (WCNC), pages 100-106, March 2005.

[5] G. Bianchi. Performance analysis of the IEEE 802.11 distributed coordination function. IEEE Journal on Selected Areas in Communications, Volume 18(3), pages 535-547, 2000.

[6] J. Camp, E. Aryafar and E. Knightly. Coupled 802.11 Flows in Urban Channels: Model and Experimental Evaluation. In INFOCOM, San Diego, CA, March 2010.

[7] A. Kherani, R. El-Khoury, R. El-Azouzi and E. Altman. Stability-throughput tradeoff and routing in multi-hop wireless ad-hoc networks. Computer Networks, volume 52(7), pages 1365-1389, 2008.

[8] A. Kumar, E. Altman, D. Miorandi and M. Goyal. New insights from a fixed point analysis of single cell IEEE 802.11WLANs. In INFOCOM, pages 1550-1561, 2005.

[9] N. Li, J. C. Hou and L. Sha. Design and analysis of a MST-based distributed topology control algorithm for wireless ad-hoc networks. IEEE Transactions on Wireless Communications, volume 4(3), pages 1195-1207, 2005.

[10] K. Medepalli and F.A.Tobagi. Towards performance modeling of IEEE 802.11 based wireless networks: A unified framework and its applications. In Proceedings of IEEE INFOCOM, 2006.

[11] V. Ramaiyan, A. Kumar and E. Altman. Fixed point analysis of single cell IEEE 802.11e WLANs: uniqueness, multistability and throughput differentiation. SIGMETRICS Performance Evaluation Review, Volume 33(1), pages 109-120, 2005.

[12] He, J., and Pung H.K.: Performance modelling and evaluation of IEEE 802.11 distributed coordination function in multihop wireless networks. Computer Communications, 29(9):1300-1308, 2006.

[13] T. Sakurai and H.L. Vu. Mac access delay of IEEE 802.11 DCF. IEEE Transactions on Wireless Communications, volume 6(5), pages 1702-1710, 2007.

[14] Vassis, D., and Kormentzas, G.: Performance analysis of IEEE 802.11 ad hoc networks in the presence of hidden terminals. Computer Networks, 51(9):2345-2352, 2007.

[15] Vassis, D., and Kormentzas, G.: Performance analysis of IEEE 802.11 ad hoc networks in the presence of exposed terminals. Ad Hoc Networks, Volume 6(3), pages 474-482, 2008.

[16] Yang, Y., Hou, V., and Kung, L.C.: Modeling the effect of transmit power and physical carrier sense in multi-hop wireless networks. In Proceedings of IEEE INFOCOM, 2007.

[17] Zhu, Y., Huang, M., Chen, S. Wang, Y.: Cooperative energy spanners: Energy-efficient topology control in cooperative ad hoc networks. In Proceedings IEEE of IEEE INFOCOM, Pages 231-235, Shanghai, China, 10-15 April 2011.

[18] Li, C., and Dai, H.: On the Throughput Scaling of Cognitive Radio Ad Hoc Networks. In proceeding of INFOCOM, , Pages 241-245, Shanghai, China, 10-15 April 2011.

[19] Chu X., and Sethu, H.: Cooperative Topology Control with Adaptation for Improved Lifetime in Wireless Ad Hoc Networks. In Proceedings IEEE of IEEE INFOCOM, Pages 262-270, Orlando, Florida, USA, 25-30 March 2012.